

## Studying the self-healing reaction based on zirconium silicide in the Thermal Barrier Coating system

Z. I. Zaki<sup>a,b,\*</sup>, Q. Mohsen<sup>a</sup>, S. H. Alotaibi<sup>c</sup> and M. H. El-Sadek<sup>b</sup>

<sup>a</sup>Material Science and Engineering Group, Chemistry Department, Faculty of Science, Taif University, Taif, Saudi Arabia

<sup>b</sup>Central Metallurgical Research and Development Institute (CMRDI), Helwan, Egypt

<sup>c</sup>Department of Chemistry, Faculty of Turabah University College, Taif University, Turabah 21995, Saudi Arabia

This work investigated the behaviour of introducing ZrSi<sub>2</sub> layer between the top coat layer Yttria-stabilized zirconia (YSZ) and the bond coat layer CoNiCrAlY in thermal barrier coatings where ZrSi<sub>2</sub> layer helped self-healing of the cracks. Powder mixtures of ZrSi<sub>2</sub>/8YSZ and ZrSi<sub>2</sub>/CoNiCrAlY were used to imitate the real case. At 800 °C under argon, there was no change in the chemical composition of both ZrSi<sub>2</sub> and 8YSZ. ZrSi<sub>2</sub> was oxidized in case of treatment in air atmosphere at 800 °C with no evidence for any self-healing reactions. At 1000 and 1200 °C under argon the formation of ZrSiO<sub>4</sub> phase was detected which was a strong evidence of self-healing reaction. ZrSiO<sub>4</sub> phase was also detected at 1200 °C in air with the appearance of SiO<sub>2</sub> phase. A limited interaction was detected at 1000 °C between ZrSi<sub>2</sub> and CoNiCrAlY under vacuum. Si was detected in the surface of CoNiCrAlY grains and Ni was detected in the composition of ZrSi<sub>2</sub>. This behavior could contribute to a chemical bonding between ZrSi<sub>2</sub> and CoNiCrAlY layers. The obtained data were confirmed by XRD, SEM and EDX analyses.

**Key words:** Self-healing, zirconium silicide, thermal barrier coatings.

### Introduction

Hot components in engines are protected with thermal barrier coatings (TBCs), and its demand has increased as gas turbine engines have been improved [1]. This improvement consists of a higher gas steam working temperature, and this implies the need to protect blades in order to increase their lifetime. TBCs are mainly composed of a ceramic top coat based on yttria partially stabilized zirconia as insulator and an interlayer of MCrAlY (M: Ni, Co) as bond coat (BC). The latter is used to improve the bond between the metallic part and the top coat, and also to provide protection against oxidation and hot corrosion [2]. The coating is also used to protect the superalloy substrate against mechanical damages [3]. During high temperature operations a thermally grown oxide (TGO) layer is developed between the BC and TBC, which acts as a diffusion barrier for oxygen. Rabiei stated that the blade's lifetime is limited by this oxide scale rather than because of part failure [4].

The interface regions undergo high stresses due to the mismatch of thermal expansion between bond coat and TBC. Additional growth stresses due to the development of TGO and stresses caused by interface roughness are also superimposed. During cooling (thermal

cycling) stresses are accumulated, which results in early crack initiation at the bond coat/TGO interface and spallation failure afterwards. Such spallation of the TBC will reduce the lifetime of the coated components in turbine engines [4-6]. It was also reported that during cooling the martensitic phase transformation from tetragonal to monoclinic was developed which may contribute to crack initiation [7].

Researchers have attempted to improve TBC lifetime by employing dense Yttria-stabilized zirconia YSZ coating structures under very low pressure plasma spray (VLPPS), electrodepositing, laser re-melting [8-10] and air plasma spray coating [3]. The dense nanostructure of YSZ layers plays an effective role in reducing oxygen permeation [9], and creates a TBC with favorable thermal shock resistance due to reduced TGO growth in the YSZ/BC interface [10]. Nano-structured SiC was also used to reinforced TBCs based on zirconia [11].

Recently, the self-healing of cracks comes into the focus as a new repairing concept. Self-healing is the capacity of a system to repair damage by itself so that cracks are sealed [12]. Self-healing materials include polymers [13], metals [14], ceramics [15] and their composites [16] that when damaged through thermal, mechanical, ballistic, or other means have the ability to restore their own original properties [17]. Self-healing materials are often used to produce anticorrosion coatings [18]. Self-healing can improve the longevity and safety of various structures [19]. In 1970s, ceramic

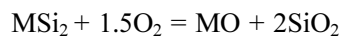
\*Corresponding author:  
Tel : +966590019562  
E-mail: zakimohamed2000@yahoo.com

materials' self-healing was first reported [20] which could heal the cracks in ceramic using heat treatment. Over past few years, many reports had been published about self-healing material of polymers, metal and concrete [21]. The National Aeronautics and Space Administration (NASA) published a detailed report about high temperature lightweight self-healing composites, which included CrSi<sub>2</sub>, CrMoSi and MoSi<sub>2</sub> for aircraft engine applications [22]. TiC has been reported as self-generating in situ phase which can improve the oxidation resistance of superalloy [23].

Self-healing of cracks is the most recent trend in solving TBC spallation problems through increasing the lifetime of the gas turbine blades [24-26]. A self-healing concept introduces an additional silicide layer to the TBCs system between the bond coat and the top coat layers. For the component to reach lifetimes of the order of many thousands of hours at high temperature in oxidizing and corrosive environments, as typically required for TBC systems of advanced jet engines, self-healing must be introduced. Few publications were found in the literatures which were related to self-healing of cracks in TBC systems. Disilicide of molybdenum, MoSi<sub>2</sub>, was previously investigated as a self-healing agent of TBC systems. Sonoya et al [27] stated that using MoSi<sub>2</sub> as a self-healing agent rose the thermal cycles of TBC from 20 to 60 cycles which meant a three-fold increase in lifetime of the component. Derelioglu [28] showed that the oxidative decomposition of MoSi<sub>2</sub> embedded in a TBC at high temperatures led to the formation of amorphous SiO<sub>2</sub> which flowed into cracks and established direct contact with the crack faces. The wetting of the crack faces was followed by a chemical reaction with the ZrO<sub>2</sub> based TBC coating leading to the formation of solid ZrSiO<sub>4</sub>. This chemical reaction generated a strong bonding between healing agent and matrix material and resulted in a complete filling and sealing of the crack [28]. In a parallel study, Frank stated that zircon is observed far away from the MoSi<sub>2</sub> particles and this can be very beneficial for the self-healing mechanism of the composite [29]. TiC was also investigated as a self-healing in TBC systems [26]. TiC was inserted between the top coat and bond coat layers and pre-treated in air atmosphere at 600 °C. TiC acted as a self-healing agent releasing its oxide (TiO<sub>2</sub>) by reaction with oxygen in air and heals the cracks/pores present in the coatings [26].

The self-healing of crack depends mainly on the oxidation products of the silicide layer. Silicides usually oxidize and liberate silica and metal oxides (MO)

according to the following equation [30].



When cracks in the TBC propagated and reached the silicide layer, the silicides of metals MSi<sub>2</sub> starts to oxidize due to its interaction with the penetrated oxygen giving rise to SiO<sub>2</sub>. The liberated SiO<sub>2</sub> then fills the cracks and chemically bonded to the cracks' sides due to the reaction between silica and zirconia with the formation of zircon: ZrO<sub>2</sub> + SiO<sub>2</sub> = ZrSiO<sub>4</sub>. Therefore, the efficiency of healing will depend on the rate of SiO<sub>2</sub> formation during the oxidation of silicide [31].

This work aims at investigating the possibility of introducing ZrSi<sub>2</sub> layer between the top coat layer 8YSZ and the bond coat layer CoNiCrAlY of the thermal barrier system. This aim is organized to be achieved by studying the anticipated interactions of ZrSi<sub>2</sub> with 8YSZ and ZrSi<sub>2</sub> with CoNiCrAlY as powder mixtures at high temperatures. The effect of temperature will be studied and a full concept about the possibility of using ZrSi<sub>2</sub> as intermediate layer for self-healing will be introduced.

## Research Methodology

The materials used in this study are given in the Table 1.

Both 8YSZ and CoNiCrAlY were provided by Saudi Aramco Company which were used by Aramco in coating processes. The powders were weighed in 1:1 per weight ratio and were mixed in agate mortar and dry blended in a slow rotating mill with zirconia balls for 5 h. The powder mixture was uniaxially pressed without binder at 78 MPa into cylindrical compact of 1.0 cm height and 1.0 cm diameter.

The compact was transferred to a muffle furnace. In some experiment the compacts were treated in a tube furnace in a controlled atmosphere of argon. The temperature of the furnace was then adjusted at the desired value (800 ~ 1,200 °C) and the treatment was carried out for 2 h. In some experiments, the compact was put into a silica tube which then evacuated and sealed.

Different phases of the products were identified by X-ray diffraction analysis using X-ray diffractometer (D8 Advanced Bruker AXS, GmbH, karlsruhe, Germany). Microstructure of specimens was investigated using Scanning Electron Microscope (SEM, Model JSM-5410, JEOL, Tokyo, Japan) equipped with electron dispersive

**Table 1.** Properties of the materials used in this study.

Powder	Chemical formula	Purity, %	Mean particle size, μm & Shape	Company
AMDRY 995 C	CoNiCrAlY	98.5	35,13.5,8.3,1.5 spherical	Oerlikon-Metco, USA
Zirconium silicide	ZrSi <sub>2</sub>	99	<20	Sigma-Aldrich, USA
Yttria-stabilized zirconia	8YSZ	99	<20 spherical	Oerlikon-Metco, USA

spectroscopy (EDX). The samples were coated with gold to ensure good electrical conductivity of the entire components of the sample.

## Results and Discussion

### Studying the reaction between $ZrSi_2$ and 8YSZ

This series of experiments was conducted in order to study the reaction between  $ZrSi_2$  and 8YSZ in air and argon atmospheres. According to the geometry of the coatings, the proposed  $ZrSi_2$  layer lays between the top layer (YSZ) and the bond coat one (CoNiCrAlY). Although the top layer completely isolates the  $ZrSi_2$  layer from air, some oxygen from the air can penetrate the top zirconia layer through generated cracks and attacks the  $ZrSi_2$  layer. Therefore, this series of experiments was carried out under argon and air using a blend of 8YSZ and  $ZrSi_2$  powders at different temperatures (800 ~ 1200 °C) for 2 h.

### Studying the reaction between $ZrSi_2$ and 8YSZ under argon

This series of experiments was devoted for studying the possible reaction between  $ZrSi_2$  and 8YSZ powders at different temperatures (800 ~ 1,200 °C) for 2 h under argon. The blend was pressed into cylindrical compacts of 1.0 cm diameter and 1.0 cm length. Generally, XRD of the samples treated at 800, 1,000 and 1,200 °C, Fig. 1, showed the presence of YSZ and  $ZrSi_2$  as the main phases and traces of monoclinic zirconia. No evidences for the formation of zirconium silicate  $ZrSiO_4$  or silica was observed in the XRD pattern of the sample treated at 800 °C. This indicated that there was no interaction or that it could be a low interaction between  $ZrSi_2$  and YSZ at this temperature. XRD of the sample treated at

1,000 and 1,200 °C showed the appearance of diffraction pattern of ( $ZrSiO_4$ ) a minor and moderate phase, respectively. The formation of zirconium silicate  $ZrSiO_4$  proved the oxidation of  $ZrSi_2$  to  $ZrO_2$  and  $SiO_2$  with the interaction of the product with YSZ. Although the study was carried out under argon atmosphere, but still there was a chance of some oxygen traces contaminating the argon gas to oxidize  $ZrSi_2$  and produced silica which in turn reacted with YSZ and finally produced  $ZrSiO_4$ . The formation of zirconium silicate  $ZrSiO_4$  was a good indication for the occurrence of self-healing as explained at the introduction section [28, 31].

SEM investigations of the sample treated under argon at 1,000 °C and 1,200 °C is given in Fig. 2. It could be seen that there was no big difference between the microstructures of the two samples. 8YSZ was appeared in its spherical shape while  $ZrSi_2$  appeared in irregular particles shapes. Generally, EDX analysis of the irregular shape particles ( $ZrSi_2$ ) gave information about the oxidation behavior of  $ZrSi_2$  while EDX analysis of spherical shape particles reflected the degree of interaction between the oxidation product of  $ZrSi_2$  and YSZ. EDX analysis of spherical shape particles of the sample treated at 1,000 °C, Fig. 3, showed that the main composition was Zr and O with the presence of small amounts of Si in the compositions. This is a good indication of the formation of  $ZrSiO_4$  on the surface of 8YSZ. This ensured that the interaction between the oxidation product of  $ZrSi_2$  and 8YSZ was occurred at this temperature. The oxidation of  $ZrSi_2$  could be due to the oxygen contamination of the argon gas which was used as inert atmosphere. EDX analysis of the irregular shape particles of the sample treated at 1,000 °C, Fig. 4, showed that these particles were

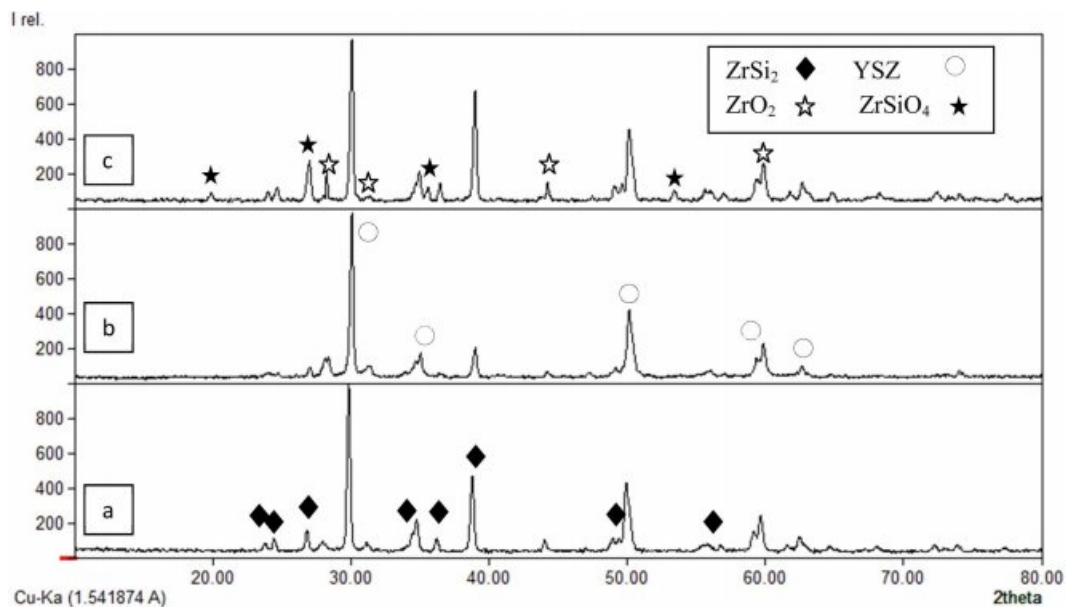


Fig. 1. XRD pattern of the samples treated under argon at different temperatures: (a) 800 °C, (b) 1,000 °C, (c) 1,200 °C.

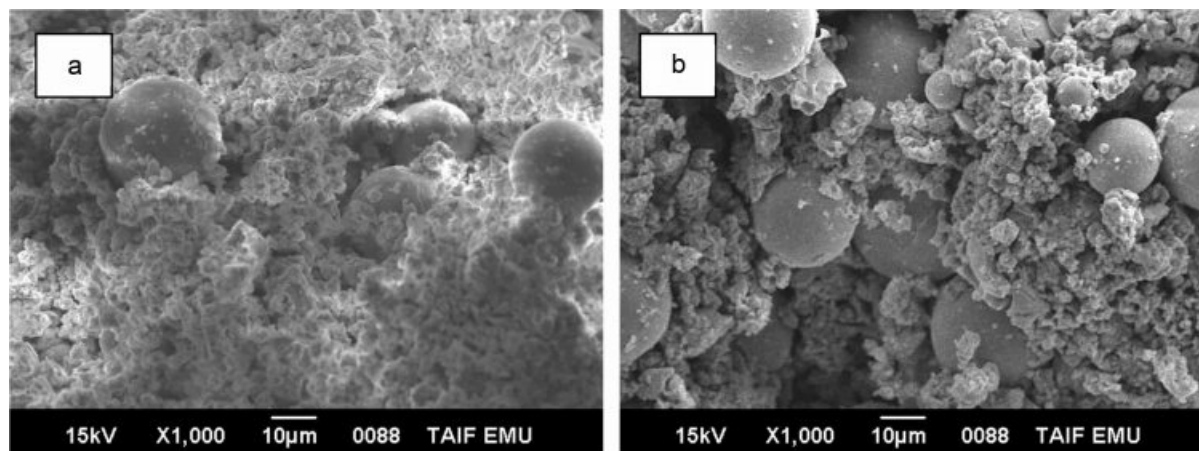


Fig. 2. SEM images of the samples treated under argon at: (a) 800 °C, (b) 1,000 °C, (c) 1,200 °C.

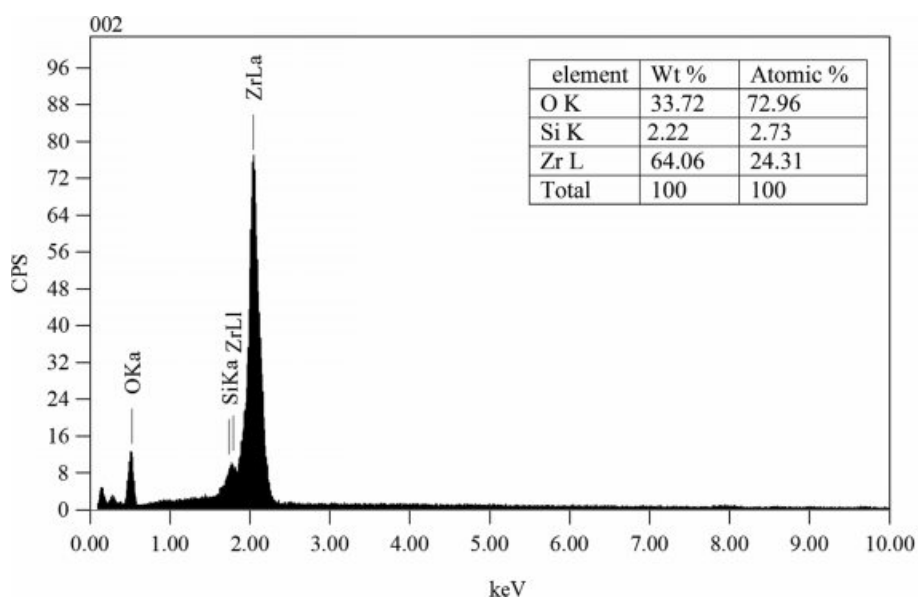


Fig. 3. EDX analysis of the sample treated under argon at 1,000 °C, spherical shape particles.

mainly composed of Zr, Si and O. The oxygen was present in appreciable amounts. This also proved that there was a degree of interaction between the  $ZrSi_2$  and the oxygen contamination of the inert gas (argon). At 1,200 °C, there was a noticeable increase in the mass % of Si of the spherical shape particles (21.24 wt %) compared with that (2.22 wt %) of the sample treated at 1,000 °C. This indicated a higher degree of interaction between the oxidation product of  $ZrSi_2$  and YSZ.

### Studying the reaction between $ZrSi_2$ and 8YSZ in air

This series of experiments was devoted for studying the possible reaction between 8YSZ and  $ZrSi_2$  powders (1 : 1 wt ratio) at different temperatures (800 ~ 1,200 °C) in air atmosphere for 2 h. XRD of the sample treated in air at 800, 1,000 and 1,200 °C showed the presence of YSZ as the main phase, Fig. 5. The diffraction pattern of  $ZrSi_2$  was completely disappeared. The

diffraction pattern of monoclinic zirconia was also detected as minor phase. This meant that  $ZrSi_2$  was completely oxidized at these conditions. No evidence for the formation of zirconium silicate  $ZrSiO_2$  or silica was monitored in the XRD pattern of the sample treated at 800 and 1000 °C in air. The free energies of  $ZrSiO_4$  formation from  $ZrO_2$  and  $SiO_2$  at 800 and 1,000 °C have a negative values (-9.96 and -7.6 KJ/mol respectively) which is good evidence for the reaction occurrence. However, the absence of  $ZrSiO_4$  at these temperatures suggested that the formation reaction proceeded with very low rate. This is in accordance with the previous studies which reported the formation of zircon ( $ZrSiO_4$ ) from  $ZrO_2$  and  $SiO_2$  at temperatures as low as 1,200 °C [32] and at a thermal treatment at 1,450 ~ 1,500 °C in air [33]. This meant that the oxidation of  $ZrSi_2$  at 800 and 1,000 °C was preceded with the formation of silicon monoxide gas (SiO) instead of silica according to reaction (1):

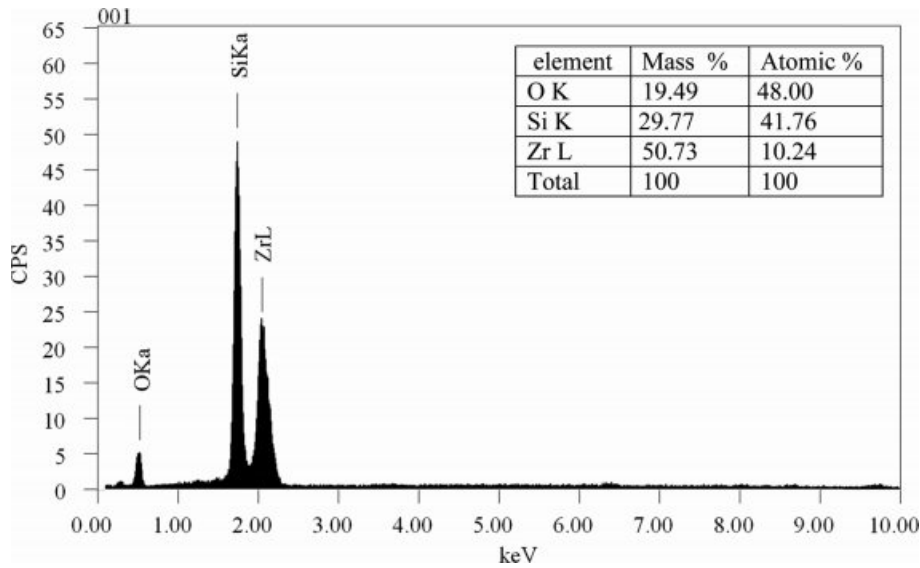


Fig. 4. EDX analysis of the sample treated under argon at 1,000 °C, irregular shape particles.

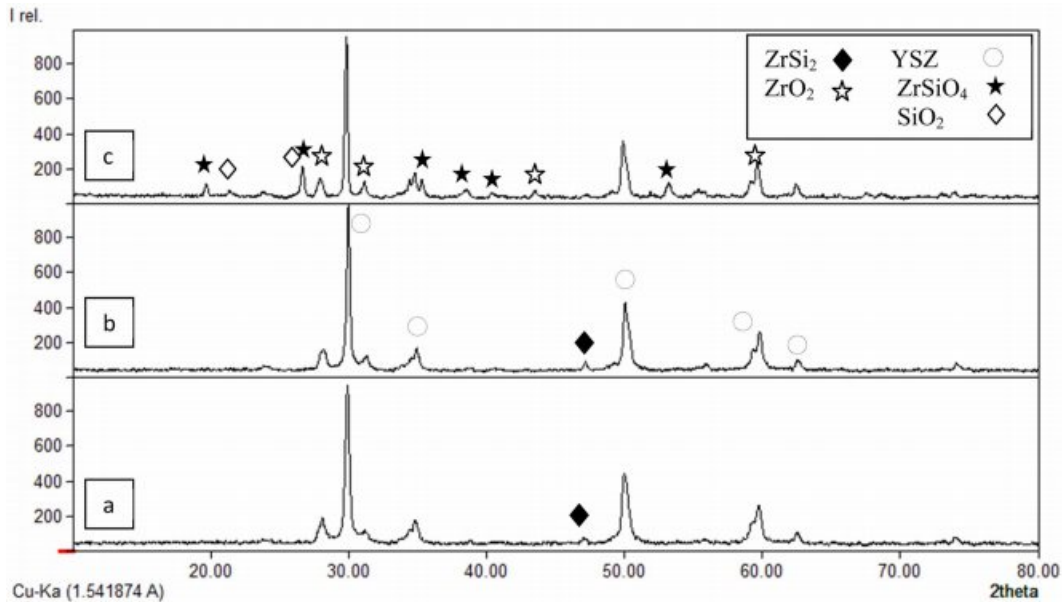
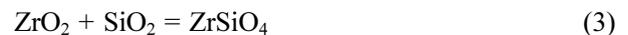


Fig. 5. XRD of the sample (8YSZ and ZrSi<sub>2</sub> mix) treated in air at: (a) 800 °C, (b) 1,000 °C, (c) 1,200 °C.



On the other hand XRD of the sample treated in air at 1,200 °C showed the diffraction pattern of silica (SiO<sub>2</sub>) and the diffraction pattern of ZrSiO<sub>4</sub> were appeared. The appearance of the diffraction pattern of silica SiO<sub>2</sub> proved the oxidation of ZrSi<sub>2</sub> to ZrO<sub>2</sub> and SiO<sub>2</sub> according to reaction (2):



The formation of zirconium silicate (ZrSiO<sub>4</sub>) indicated the interaction of the produced silica SiO<sub>2</sub> with ZrO<sub>2</sub> content of YSZ according to reaction (3):

SEM investigations of the sample treated at 1,000 °C and 1,200 °C in air are given in Fig. 6(a&b). No significant differences between the EDX analyses of spherical shape particles of the sample treated at 1,000 °C in air compared with that treated under argon. Si was also detected in a little amount (3.7 wt %) in the composition indicating the formation of ZrSiO<sub>4</sub> on the surface of 8YSZ (not detected by XRD). EDX analysis of the irregular shape particles of the sample treated at 1,000 °C in air showed increasing amounts of oxygen (39.7 wt %) compared with that under argon (19.49 wt %) with a correspondence decrease in the Si amounts from 29.77 in case of air to 19.27 wt % in case of

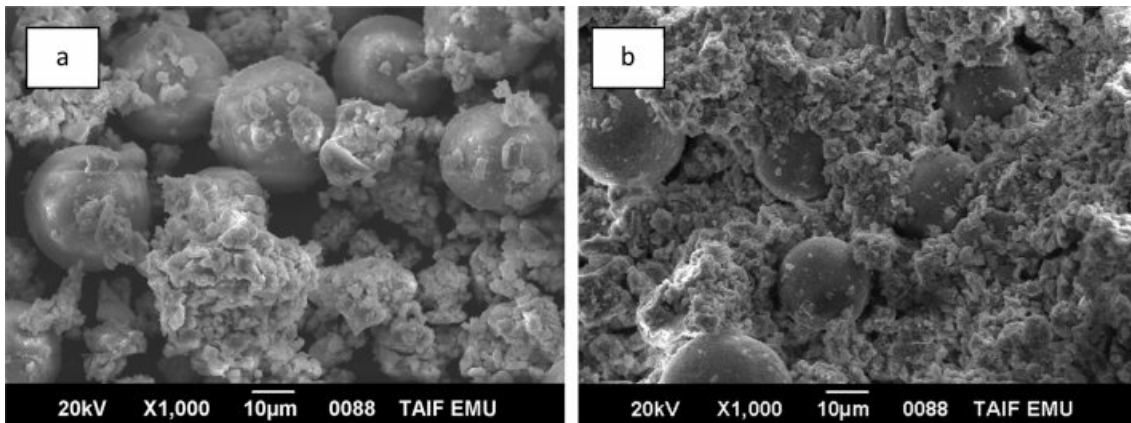


Fig. 6. SEM images of the samples treated in air at: (a) 1,000 °C and (b) 1,200 °C.

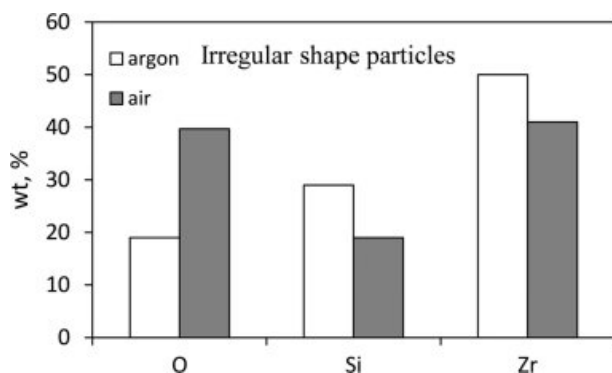


Fig. 7. EDX analyses of the samples (irregular shape particles) treated in air and under argon at 1,000 °C.

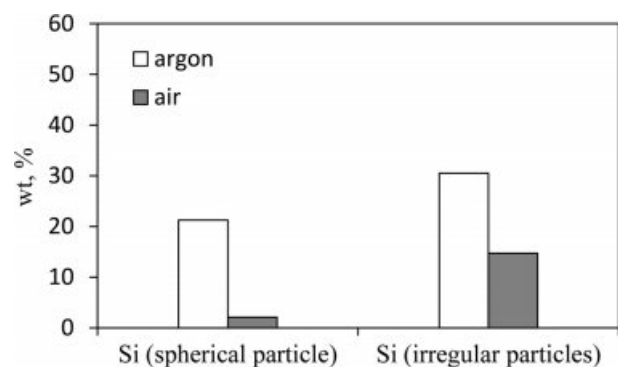


Fig. 8. EDX analyses of Si content of the sample (irregular and spherical shape particles) treated in air and under argon at 1,200 °C.

argon, Fig. 7. The decrease in silicon amounts could be due to either evaporation from the reaction media as a gas and/or its consumption in the reaction with YSZ. The detection of Si and O in the EDX analysis and the disappearance of silica in XRD investigation suggest that silica was produced in an amorphous phase or silicone monoxide gas was produced and part of it was evaporated from the sample.

EDX analysis of spherical shape particles of the sample treated in air at 1,200 °C showed a very little amount of Si (2.1 wt %) compared with that in case of argon treatment (21.24 wt %), Fig. 8. This can be related to either the very high evaporation rate of the oxidation product of  $ZrSi_2$  or the decomposition of the formed  $ZrSiO_4$ . EDX analysis of irregular shape particles of the sample treated in air at 1,200 °C showed a decrease of Si content (14.75 wt %) compared with that in case of argon treatment (30.51 wt %), Fig. 8. This result recommended that the oxidation product of  $ZrSi_2$  was spilt out the sample with a high rate. However, a newly formed phase was detected in case of 1,200 °C. The composition of this phase was free from Zr and contains only silicone and oxygen. This finding was in good accordance with XRD investigation of this sample where  $SiO_2$  was detected at 1,200 °C.

### Studying the reaction between $ZrSi_2$ and bond coat layer CoNiCrAlY

This series of experiments was devoted for studying the possible reaction between  $ZrSi_2$  and CoNiCrAlY powders, 1:1 weight ratio, at 1,000 °C for 2 h. The sample was capsulated into silica tube and treated under vacuum.

XRD of CoNiCrAlY as received powder (without any treatment) is given in Fig. 9. The diffraction pattern was mainly composed of the pattern of  $Ni_3Al$  phase and moderate intensity lines of CoAl phases. No other phases were detected. On the other hand, XRD of the sample treated at 1,000 °C showed the presence of  $ZrSi_2$  as the main phases, Fig. 9. Moderate intensity lines were detected for ZrSi phase. The diffraction pattern of  $Ni_3Al$  phase was also detected as minor phase. No evidences for the interaction between  $ZrSi_2$  and CoNiCrAlY.

CoNiCrAlY appeared in a spherical shape while the irregular shape particles consisted mainly of Zr and Si according to EDX analysis. EDX analysis of spherical shape particles of the sample treated at 1,000 °C is given in Fig. 10. The spherical shape-particle was composed mainly of Co, Ni, Al, Cr and Si. The presence of Si in the composition of CoNiCrAlY indicated that

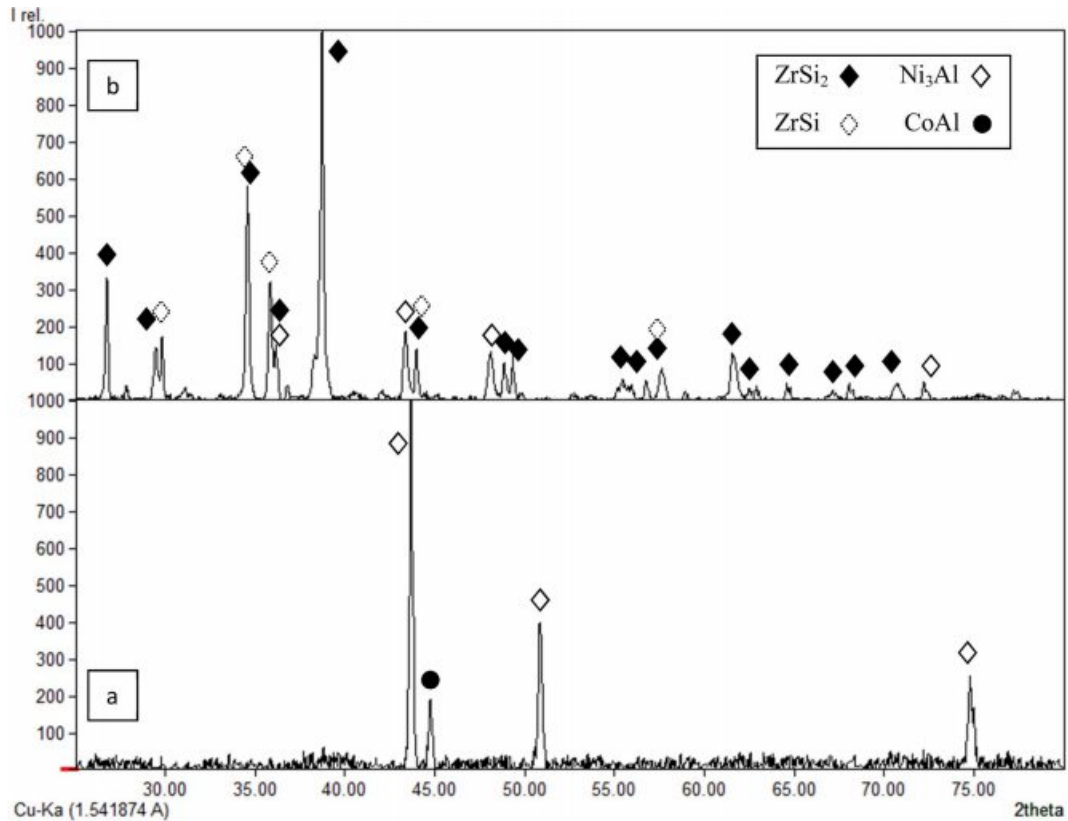


Fig. 9. XRD pattern of the samples: (a) CoNiCrAlY raw, (b) mix of ZrSi<sub>2</sub> and CoNiCrAlY powders, 1,000 °C.

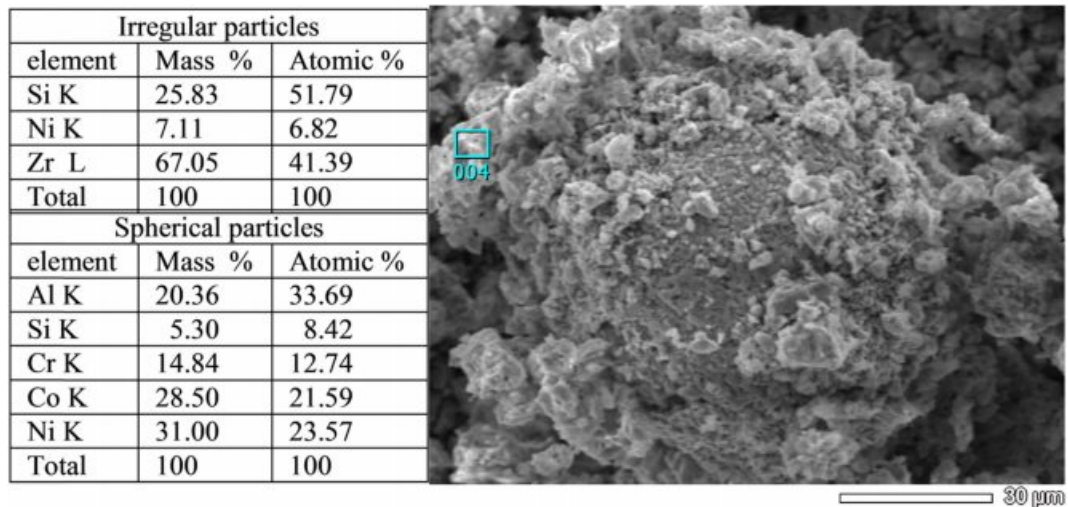


Fig. 10. SEM image and EDX analyses of the spherical and irregular shape particles treated at 1,000 °C under vacuum.

there was an interaction between CoNiCrAlY and the ZrSi<sub>2</sub> particles. On the other hand, EDX analysis of the irregular shape particles, Fig. 10, illustrated that these particles were mainly composed of Zr and Si. Traces of Ni were also detected. The presence of some Si in composition of CoNiCrAlY and the presence of some Ni in the composition of ZrSi<sub>2</sub> particles proved that there was a kind of interaction between the Si of ZrSi<sub>2</sub> and the Ni of CoNiCrAlY which contributed to an anticipated bonding between the newly introduced

layer ZrSi<sub>2</sub> and the bond coat layer CoNiCrAlY.

## Conclusion

Powder mixtures of ZrSi<sub>2</sub> with 8YSZ, and ZrSi<sub>2</sub> with CoNiCrAlY were successfully used to imitate the behavior of introducing ZrSi<sub>2</sub> layer into thermal barrier coating system at high temperatures.

At 800 °C under argon, there was no change in the chemical composition of both ZrSi<sub>2</sub> and YSZ.

At 1,000 and 1,200 °C under argon the formation of ZrSiO<sub>4</sub> phase was detected which was a strong evidence of self-healing reaction. ZrSiO<sub>4</sub> phase was only detected in little amounts at 1,200 °C in air with the appearance of SiO<sub>2</sub> phase.

The entire amount of ZrSi<sub>2</sub> was oxidized in case of air treatment at 800, 1,000 and 1,200 °C.

At 1,000 °C under vacuum, Si was detected in the surface of CoNiCrAlY and Ni was detected in the composition of ZrSi<sub>2</sub>. This behavior can contribute to an anticipated chemical bonding between ZrSi<sub>2</sub> and CoNiCrAlY layers in the real case of thermal barrier coating.

### Acknowledgment

The authors would like to express their gratitude for Taif University, KSA for funding this project under the grant no. 5237-437.

### References

1. N. Nayeypashaeaa, S.H. Seyedeina, M.R. Aboutaleb, H. Sarpoolakyb, and M.M. Hadavic, *J. Ceram. Process. Res.* 17[8] (2016) 803-814.
2. V. Crespo, I.G. Cano, S. Dosta, and J.M. Guilemany, *J. Alloys Compd.* 622 (2015) 394-401.
3. L. Dong Heon, J. Bin, K. Chul, and L. Kee Sung, *J. Ceram. Process. Res.* 20[5] (2019) 499-504.
4. A. Rabiei and A.G. Evans, *Acta Mater.* 48[15] (2000) 3963-3976.
5. P. Poza, J. Gómez-García, and C.J. Múnez, *Acta Mater.* 60[20] (2012) 7197-7206.
6. G. Bolelli, A. Candeli, L. Lusvardi, A. Ravoux, K. Cazes, A. Denoirjean, S. Valette, C. Chazelas, E. Meillot, and L. Bianchi, *Wear* 344-345 (2015) 69-85.
7. M. Jaeyun, C. Hanshin, L. Changhee, *J. Ceram. Process. Res.* 1[1] (2000) 69-73.
8. F. Li, X. Jiang, J. Zhao, and S. Zhang, *Nano Energy* 16 (2015) 488-515.
9. N. Narimani and M. Saremi, *Ceram. Int.* 41[10, Part A] (2015) 13810-13816.
10. L. Zhu, N. Zhang, R. Bolot, H. Liao, and C. Coddet, *Surf. Rev. Lett.* 22[05] (2015) 1550061.
11. L. Joo Won, L. Chang Hee, and K. Hyung Jun, *J. Ceram. Process. Res.* 2[3] (2001) 113-119.
12. F. Rebillat, in "Advances in Ceramic Matrix Composites" (Woodhead Publishing, 2014) pp. 369-409.
13. P. Cordier, F. Tournilhac, C. Soulie-Ziakovic, and L. Leibler, *Nature* 451[7181] (2008) 977-980.
14. V. Amendola, D. Dini, S. Polizzi, J. Shen, K.M. Kadish, M.J.F. Calvete, M. Hanack, and M. Meneghetti, *J. Phys. Chem. C* 113[20] (2009) 8688-8695.
15. H. Mihashi and T. Nishiwaki, *ACT* 10[5] (2012) 170-184.
16. M. Krogsgaard, M.R. Hansen, and H. Birkedal, *J. Mater. Chem. B* 2[47] (2014) 8292-8297.
17. R.P. Wool, *Soft Matter* 4[3] (2008) 400-418.
18. D.V. Andreeva, D. Fix, H. Möhwald, and D.G. Shchukin, *Adv. Mater.* 20[14](2008) 2789-2794.
19. E. Bouillon, F. Abbe, S. Goujard, E. Pestourie, G. Habarou, and B. Dambrine, in 24th Annual Conference on Composites, Advanced Ceramics, Materials, and Structures: A: Ceramic Engineering and Science Proceedings, March 2008, edited by T. Jessen (John Wiley & Sons, Inc., 2008) p. 459.
20. F.F. Lange and T.K. Gupta, *J. Am. Ceram. Soc.* 53[1] (1970) 54-55.
21. S.K. Ghosh, in "Self-Healing Materials" (Wiley-VCH Verlag GmbH & Co. KGaA, 2009) pp. 1-28.
22. S.V. Raj, M. Singh, and R.T. Bhatt, *NASA* (2014).
23. B. Ya, B. Zhou, H. Yang, B. Huang, F. Jia, and X. Zhang, *J. Alloys Compd.* 637 (2015) 456-460.
24. A. Lutz, J.M.C. Mol, I. De Graeve, and H. Terryn, in "Smart Composite Coatings and Membranes" (Woodhead Publishing, 2016) p. 157.
25. T. Ouyang, X. Fang, Y. Zhang, D. Liu, Y. Wang, S. Feng, T. Zhou, S. Cai, and J. Suo, *Surf. Coat. Technol.* 286 (2016) 365-375.
26. T. Ouyang, J. Wu, M. Yasir, T. Zhou, X. Fang, Y. Wang, D. Liu, and J. Suo, *J. Alloys Compd.* 656 (2016) 992-1003.
27. K. Sonoya, M. Nakamura, and M. Sekine, in *Power Engineering and Optimization Conference (PEOCO), IEEE International 8th, March 2014* (Institute of Electrical and Electronics Engineers, 2014) p. 13.
28. Z. Derelioglu, A.L. Carabat, G.M. Song, S.v.d. Zwaag, and W.G. Sloof, *J. Eur. Ceram. Soc.* 35[16] (2015) 4507-4511.
29. F. Nozahic, D. Monceau, and C. Estournès, *Materials & Design* 94 (2016) 444-448.
30. Z.I. Zaki, N.Y. Mostafa, and Y.M.Z. Ahmed, *Int. J. Refract. Met. Hard Mater.* 45 (2014) 23-30.
31. V. Kochubey and W.G. Sloof, in *Self healing mechanism in thermal barrier coatings, 2008* (In: ITSC proceedings, 2008).
32. Musyarofah, R. Nurlaila, N.F. Muwwaqor, M. Saukani, A. Kuswoyo, Triwikantoro, and S. Pratapa, *Journal of Physics: Conference Series* 817 (2017) 012033.
33. A.A. Ballman and R.A. Laudise, *J. Am. Ceram. Soc.* 48[3] (1965) 130-133.